

**ATTENUATION OF ELECTROMAGNETIC ACOUSTIC NOISE FROM A
VARIABLE SPEED INDUCTION MOTOR BY USING DYNAMIC
VIBRATION ABSORBER**

by

VIGREN A/L V.RADHA

**Thesis submitted in fulfillment of the requirements
for the degree of
Master of Science**

March 2016

ACKNOWLEDGEMENTS

A million thanks to Prof. Zaidi bin Mohd. Ripin for supervising me for my Masters degree. Without his guidance this thesis will not be possible. I remember the times that I was lost and clueless in my research direction. Your guidance support made me on track again and to finally able to complete my research successfully. Apart from your technical advice, I am also grateful for all the life lessons and philosophical aphorisms that you have shared with me.

Thanks to Prof. Horizon Walker Gitano-Briggs for inspiring my curiosity and motivating me to continue my studies. Thanks to technicians Mr. Wan Amri, Mr. Baharom Awang , Mr. Zalmi Yop, Mr. Ahmad Shauki, Mr. Jamaluddin Che Mat and also Mr. Nazir for their technical assistance. Thanks to USM office staff Pn. Farah Hamid, Pn. Wan Zahida, Pn.Bayzura and Pn.Afzan for managing my candidature matters. Many thanks to Dr. Najib Ab. Hamid and Dr. Tan Yeow Chong who have assisted me when I first came to Vibration Lab. Thanks to Dr. Devarajan Ramasamy, Dr. Ooi Lu Ean, Dr. Teoh Choe Yung, Dr. Chuah Han Guan, Dr. Tan Wei Hong, Teoh Yew Heng, Khoo Aik Soon, Lee Jih Houh, Goh Chin Yuan, Cham Chin Long, Lee Ying Wei, Chan Ping Yi, Wong Chee Koon, Syazli, Zhafran, Rabani, Izuddin, Sahlan, Farhana, Umami, Mas and CC Leong for their friendship.

To my parents, Mr. Radha Valliappan and Raja Rajeswari thanks for bringing up and nurturing me. Thanks to my aunt, Ms. Boovaneswari Govindasamy who had supported my education for as long as I can remember. Finally, I would like to express my deepest gratitude to my beloved sister Ms. Kodieswari Radha who had provided me moral and financial support throughout my Masters degree at USM.

TABLE OF CONTENTS

| | |
|-----------------------------|------|
| Acknowledgements | ii |
| Table of Contents | iii |
| List of Tables | vi |
| List of Figures | vii |
| List of Abbreviations | xiv |
| List of Symbols | xv |
| Abstrak | xvi |
| Abstract | xvii |

CHAPTER 1 - INTRODUCTION

| | |
|-----------------------------|---|
| 1.1 Overview | 1 |
| 1.2 Problem Statement | 5 |
| 1.3 Motivation | 5 |
| 1.4 Objective | 6 |
| 1.5 Contributions | 6 |
| 1.6 Scope | 7 |
| 1.7 Outline | 7 |

CHAPTER 2 - LITERATURE REVIEW

| | |
|--|----|
| 2.1 Overview | 8 |
| 2.2 Noise Generation Mechanism | 8 |
| 2.3 Electromagnetic Noise Attenuation Method | 10 |
| 2.3.1 Electromechanical Design | 10 |
| 2.3.2 Pulse Width Modulation (PWM) Strategy | 13 |
| 2.3.3 Other Methods | 16 |
| 2.4 Dynamic Vibration Absorber | 17 |
| 2.4.1 Theory | 17 |
| 2.4.2 DVA Application Examples | 21 |

| | |
|-------------------|----|
| 2.5 Summary | 25 |
|-------------------|----|

CHAPTER 3- METHODOLOGY

| | |
|--|----|
| 3.1 Overview | 27 |
| 3.2 Induction Motor and Inverter Specifications | 27 |
| 3.3 PWM Waveform Tracing..... | 29 |
| 3.4 Noise and Vibration Characterization | 30 |
| 3.4.1 Spectral Test..... | 31 |
| 3.4.2 Experimental Modal Analysis (EMA) | 33 |
| 3.4.3 Operational Deflection Shape (ODS) Analysis..... | 35 |
| 3.4.4 DVA Experimental Modal Analysis | 37 |
| 3.4.5 Motor FRF Validation..... | 39 |
| 3.5 DVA Implementation | 41 |
| 3.5.1 Effectiveness at location A, B, C and D..... | 41 |
| 3.5.2 DVA Vibration Correlation..... | 43 |
| 3.5.3 Sound Pressure Level Correlation..... | 44 |
| 3.5.4 Effectiveness at Variable Speed..... | 46 |
| 3.6 Section summary | 47 |

CHAPTER 4 - RESULTS AND DISCUSSIONS

| | |
|--|----|
| 4.1 Overview | 48 |
| 4.2 Characterization results | 48 |
| 4.2.1 Spectra Comparison | 48 |
| 4.2.2 Natural Frequency and Mode Shapes | 58 |
| 4.2.3 Operational Deflection Shape Animation | 62 |
| 4.2.4 DVA Characterization..... | 64 |
| 4.3 DVA Implementation | 66 |
| 4.3.1 General DVA Implementation | 66 |
| 4.3.2 Motor FRF Validation..... | 69 |
| 4.3.3 Vibration reduction at X, Y, Z and R axis | 71 |
| 4.3.4 Vibration reduction at B,C and D locations | 74 |
| 4.3.5 Surface Vibration and DVA Vibration Correlation | 77 |
| 4.3.6 Sound Pressure Level and Surface Vibration Correlation | 80 |

| | |
|--|----|
| 4.3.7 Effectiveness at Variable Speed..... | 83 |
|--|----|

CHAPTER 5 - CONCLUSION AND FURTHER WORKS

| | |
|-----------------------|----|
| 5.1 Conclusions | 86 |
|-----------------------|----|

| | |
|-------------------------|----|
| 5.2 Further Works | 87 |
|-------------------------|----|

| | |
|-----------------|----|
| References..... | 88 |
|-----------------|----|

List of Publications

LIST OF TABLES

| | Page |
|---|------|
| Table 1.1 Various types and source of acoustic noise from a variable speed induction motor (Gieras et al., 2005) | 2 |
| Table 3.1 Specifications of Induction Motor | 29 |
| Table 3.2 Specifications of Inverter | 29 |
| Table 4.1 Modes and natural frequency of motor structure | 59 |
| Table 4.2 Classification of acceleration magnitude of 80 points on motor surface at 6 kHz and speed of 0 rpm | 63 |
| Table 4.3 List of natural frequencies for DVA sample bolts | 66 |
| Table 4.4 Changes on the 6 kHz frequency component of the surface vibration spectrum for different lengths of bolt samples | 69 |
| Table 4.5 Surface vibration reduction percentage on all four locations at different axis | 75 |
| Table 4.6 Comparison of decrease in motor surface vibration and increase in DVA vibration | 80 |
| Table 4.7 Sound pressure level reduction at location X1, X2 and R1 upon DVA attachment | 82 |
| Table 4.8 Summary of surface vibration reduction at various motor speeds | 83 |

LIST OF FIGURES

| | | Page |
|------------|---|------|
| Figure 1.1 | Exploded view of an induction motor. (1-Front end shield, 2 - Bearing, 3 – Cage rotor, 4 - Stator, 5 – Housing, 6 – Rear end shield 7- Cooling Fan, 8- Fan Cowl) (Wildi, 2002) | 1 |
| Figure 1.2 | Maximum permissible Sound Power Levels in Decibels for IEC Squirrel Cage Induction motors (Toliyat and Kliman, 2004) | 4 |
| Figure 2.1 | Radial Maxwell magnetic force (F_R) and tangential magnetic force (F_T) in the air gap. (Pyrhönen et al., 2008) | 8 |
| Figure 2.2 | Mechanism for electromagnetic noise generation in induction motor (Gieras et al., 2005) | 9 |
| Figure 2.3 | Image of (a) Unskewed rotor (b) Skewed rotor (Kubicek et al., 2009) | 12 |
| Figure 2.4 | Figure 2.4 (a) Typical PWM is generated from comparison of sine wave and triangular wave (Kükrer, 2000) (b) Comparison of harmonics spectrum (i) typical PWM (ii) random PWM (Lai and Chen, 2013) | 15 |
| Figure 2.5 | Spring-mass system model to represent the DVA theory (Zill et al., 2011) | 18 |
| Figure 2.6 | Theoretical model of the panel for DVA attachment(Sun et al., 1996) | 20 |
| Figure 2.7 | The cylindrical shell and the DVA attached to the shell (Huang and Fuller, 1998) | 20 |
| Figure 2.8 | Tuned Mass Damper (TMD) on Lathe Machine (Yang et al., 2010) | 22 |

| | | |
|-------------|--|----|
| Figure 2.9 | DVA attached to the fuselage of turboprop aircraft. It is tuned by changing the weights (42) and also length of beam (40) (Van Joseph,1970) | 23 |
| Figure 2.10 | Dynamic vibration absorber implemented on AC motor for angular velocity perturbation control (a) DVA (30) is attached to the AC motor (20) (b) The DVA consists of inertial mass (32), flexible spring (34) and mounting hub (36) (James et al., 1996) | 24 |
| Figure 2.11 | Application of DVA for dishwasher machine electric motor (a) Electric motor (10) with DVA (1) used in dishwasher (12) (b) DVA (1) consists of beam (20) and mass (22) attached to the motor (10) (Vukorpa et al.,1997) | 25 |
| Figure 3.1 | MarelliMotori induction motor (left) and Emerson SKA inverter (right) | 28 |
| Figure 3.2 | Electrical wiring diagram of the motor-inverter pair (1-Induction Motor & 2-Inverter) | 28 |
| Figure 3.3 | Experimental setup for PWM waveform tracing | 30 |
| Figure 3.4 | Schematic of PWM Waveform tracing experimental setup (1-Induction Motor, 2-Inverter, 3-Active Differential Probe & 4-Digital Oscilloscope) | 30 |
| Figure 3.5 | Experimental setup for spectral test | 32 |
| Figure 3.6 | Schematic of spectral test (1-Induction motor, 2-Accelerometers, 3- Microphone, 4- LMS Scadas& 5-PC) | 32 |
| Figure 3.7 | Surface vibration measurement grid | 32 |
| Figure 3.8 | Experimental setup for experimental modal analysis (a) Excitation using impact hammer (b) Motor hung in “free-free” condition using rubber band | 33 |

| | | |
|-------------|---|----|
| Figure 3.9 | Schematic of motor structure impact test (1-Induction motor, 2-Accelerometer, 3-Impact Hammer, 4-Measurement points, 5-Rubber band, 6-LMS Scadas, 7-PC) | 34 |
| Figure 3.10 | Measurement grid for modal analysis | 34 |
| Figure 3.11 | Reference accelerometer attached to point 6 on motor housing while roving accelerometer currently at point 22 during ODS analysis | 36 |
| Figure 3.12 | Schematic of operational deflection shape analysis (1-Induction motor, 2-Roving accelerometer, 3-Reference accelerometer, 4-Measurement points, 5-LMS Scadas, 6-PC) | 36 |
| Figure 3.13 | A 20mm M6 bolt attached at point 55 on motor housing during impact test for modal analysis | 37 |
| Figure 3.14 | Sample bolt lengths for impact test | 38 |
| Figure 3.15 | Impact test on a 20 mm M6 bolt | 39 |
| Figure 3.16 | Schematic of DVA impact test (1-induction motor, 2-DVA, 3-Impact Hammer, 4-Miniature Accelerometer, 5-LMS Scadas, 6-PC) | 39 |
| Figure 3.17 | Experimental setup to see changes in motor structure local FRF upon final DVA attachment. Accelerometer is attached at position R1 at Location A and impact hammer is knocked at point 37 | 40 |
| Figure 3.18 | Schematic of Motor FRF validation experiment (1- Induction Motor, 2- DVA, 3- Impact hammer, 4- Miniature accelerometer, 5- Foam, 6-LMS Scadas, 7-PC) | 41 |
| Figure 3.19 | Four different M6 threaded hole location on motor to attach DVA | 42 |

| | | |
|-------------|---|----|
| Figure 3.20 | (a) Location for surface vibration measurement. A 20mm DVA is attached and miniature accelerometer is attached at R1 (b) Illustration of various axes and their respective measurement points at Location A | 42 |
| Figure 3.21 | Schematic of motor surface vibration measurement before and after DVA at location A, B, C and D. (1-Induction Motor, 2-DVA, 3-Accelerometer, 4-LMS Scadas, 5-PC) | 43 |
| Figure 3.22 | Motor surface vibration and DVA vibration correlation measurement | 44 |
| Figure 3.23 | Schematic of motor surface vibration and DVA vibration correlation measurement (1-Induction Motor, 2-DVA, 3,4-Accelerometer, 5-LMS Scadas, 6-PC) | 44 |
| Figure 3.24 | Before and after DVA motor surface vibration and sound pressure level correlation measurement at location X1 | 45 |
| Figure 3.25 | Schematic of before and after DVA motor surface vibration and sound pressure level correlation measurement (1-Induction Motor, 2-DVA, 3-Microphone, 4-Accelerometer, 5-LMS Scadas, 6-PC) | 45 |
| Figure 3.26 | Schematic for DVA effectiveness at variable speed measurement (1-Induction Motor, 2-DVA, 3-Accelerometer, 4-Inverter, 5-LMS Scadas, 6-PC) | 46 |
| Figure 3.27 | Flowchart of methodology for research on application of DVA for induction motor electromagnetic noise suppression | 47 |
| Figure 4.1 | Spectra comparison at 0 rpm | 50 |
| Figure 4.2 | Spectra comparison at 250 rpm | 51 |
| Figure 4.3 | Spectra comparison at 500 rpm | 52 |

| | | |
|-------------|---|----|
| Figure 4.4 | Spectra comparison at 750 rpm | 53 |
| Figure 4.5 | Spectra comparison at 1000 rpm | 54 |
| Figure 4.6 | Spectra comparison at 1250 rpm | 56 |
| Figure 4.7 | Spectra comparison at 1500 rpm | 57 |
| Figure 4.8 | (a) Frequency response function (b) phase angle of the motor structure | 58 |
| Figure 4.9 | Mode 1 at 735 Hz indicates complex mode | 60 |
| Figure 4.10 | Mode 3 at 2029 Hz indicates ovaling mode (Diametral Mode 2) | 60 |
| Figure 4.11 | Mode 8 at 4534 Hz indicates wave mode (Diametral Mode 3) | 60 |
| Figure 4.12 | Diametral mode of cylindrical structure (a) Ovaling mode (b) Wave mode (Gieras et al., 2005) | 61 |
| Figure 4.13 | Sequence of ODS animation (from a to d) of motor structure at 6 kHz at speed of 0 rpm | 62 |
| Figure 4.14 | Point 49 and 65 (marked in green circle) on the motor exhibits very high vibration displacement | 63 |
| Figure 4.15 | Point 55 has threaded M6 hole for M6 DVA attachment | 64 |
| Figure 4.16 | (a) Frequency response function (b) Phase angle for various lengths of sample bolts | 65 |
| Figure 4.17 | PolyMAX stabilization diagram of 20 mm DVA | 65 |
| Figure 4.18 | Surface vibration changes for 60mm bolt | 67 |

| | | |
|-------------|--|----|
| Figure 4.19 | Surface vibration changes for 20mm bolt | 68 |
| Figure 4.20 | Surface vibration changes for 50mm bolt | 68 |
| Figure 4.21 | (a) FRF changes at location R1 of point 55 on motor housing (b) Close range view of the FRF upon 20mm bolt attachment | 70 |
| Figure 4.22 | Input-Transfer Function-Output concept for variable speed induction motor noise emission | 71 |
| Figure 4.23 | Surface vibration spectrum at y-axis before and after DVA (a) at location Y1 (b) at location Y2 | 72 |
| Figure 4.24 | Surface vibration spectrum at z-axis before and after DVA (a) at location Z1 (b) at location Z2 | 72 |
| Figure 4.25 | Surface vibration spectrum at x-axis before and after DVA (a) at location X1 (b) at location X2 | 73 |
| Figure 4.26 | Surface vibration spectrum at r-axis before and after DVA (a) at location R1 (b) at location R2 | 74 |
| Figure 4.27 | Surface vibration reduction at (a) Z2 (b) X2 and (c) R2 at location C at 1000 rpm | 76 |
| Figure 4.28 | Surface vibration reduction at (a) Z2 (b) X2 and (c) R2 at location D at 1000 rpm | 77 |
| Figure 4.29 | Comparison of (a) decrease in surface vibration of motor and (b) increase in DVA vibration at location X1 | 78 |
| Figure 4.30 | Comparison of (a) decrease in surface vibration of motor and (b) increase in DVA vibration at location R1 | 79 |
| Figure 4.31 | Comparison of (a) decrease in surface vibration of motor and (b) increase in DVA vibration at location Z1 | 79 |

| | | |
|-------------|--|----|
| Figure 4.32 | Reduction in (a) motor surface vibration and (b) sound pressure before and after DVA attachment at location X1 | 81 |
| Figure 4.33 | Reduction in (a) motor surface vibration and (b) sound pressure before and after DVA attachment at location X2 | 81 |
| Figure 4.34 | Reduction in (a) motor surface vibration and (b) sound pressure before and after DVA attachment at location R1 | 82 |
| Figure 4.35 | Surface vibration reduction at various speeds (a) 0 rpm (b) 250 rpm (c) 500 rpm | 84 |
| Figure 4.36 | Surface vibration reduction at various speed (a) 750 rpm (b) 1000 rpm (c) 1250 rpm (d) 1500 rpm | 85 |

LIST OF ABBREVIATIONS

| | |
|---------|--|
| AC | Alternating Current |
| AC-RPWM | Asymmetric Carrier Random PWM |
| EMA | Experimental Modal Analysis |
| FFT | Fast Fourier Transform |
| FRF | Frequency Response Function |
| IEC | International Electrotechnical Committee |
| ODS | Operational Deflection Shape |
| PFM | Pulse Frequency Modulation |
| PWM | Pulse Width Modulation |
| PZT | Piezoelectric Insert |
| RPPWM | Random Position Pulse Width Modulation |
| SLPWM | Slope Pulse Width Modulation |
| THD | Total Harmonic Distortion |
| TMD | Tunes Mass Damper |
| TVA | Tuned Vibration Absorber |
| UMP | Unbalanced Magnetic Pull |

LIST OF SYMBOLS

| | |
|--------------|--|
| B | Radial air gap magnetic flux density |
| E | Young's Modulus |
| F_1 | Harmonic forcing force |
| F_R | Radial Maxwell magnetic force |
| F_T | Tangential magnetic force |
| g | Gravitational acceleration |
| I | Beam second moment of inertia |
| k_1 | Stiffness of mass m_1 |
| k_2 | Stiffness of mass m_2 |
| l | Length of beam |
| m | Mass of beam |
| m_1 | Mass of primary structure |
| m_2 | Mass of dynamic vibration absorber (DVA) |
| x_1 | Displacement of primary structure |
| x_2 | Displacement of DVA |
| X_1 | Vibration amplitude of primary structure |
| X_2 | Vibration amplitude of DVA |
| \ddot{x}_1 | Acceleration of primary structure |
| \ddot{x}_2 | Acceleration of DVA |
| μ_0 | Air gap magnetic permeability |
| ω_n | Harmonic forcing force frequency |
| ω_1 | Natural frequency of primary structure |
| ω_2 | Natural frequency of DVA |

PENGURANGAN HINGAR AKUSTIK ELEKTROMAGNETIK DARIPADA MOTOR INDUKSI KELAJUAN BOLEH UBAH DENGAN MENGGUNAKAN PENYERAP GETARAN DINAMIK

ABSTRAK

Hingar akustik elektromagnetik mempunyai ciri ton hingar yang dihasilkan oleh motor induksi kelajuan boleh ubah mewujudkan suasana yang tidak selesa kepada pengendali mesin. Hingar yang berlaku pada frekuensi tinggi ini kebiasaannya berlakupada gandaan frekuensi pensuisan pada pembalik. Penyelesaian masalah hingar ini pada umumnya dicapai dengan rekabentuk elektromekanikal dan modulasi lebar denyut untuk membasmi harmonik yang menyebabkan hingar. Penggunaan penyerap getaran dinamik adalah antara alternatif yang dikaji di dalam penyelidikan ini. Ujian spektrum menunjukkan bahawa daya tindakan elektromagnetik mempengaruhi secara langsung hingar elektromagnetik yang dihasilkan oleh motor induksi. Gandaan harmonik 3 kHz pada spektrum modulasi lebar denyut berlaku juga pada spektrum getaran permukaan dan spektrum hingar. Analisis mod dan ujian spektrum menunjukkan bahawa hingar dengan frekuensi 6 kHz pada kelajuan 1250 rpm dan ke bawah adalah disebabkan oleh getaran paksa. Pada halaju di atas 1250 rpm, hingar 3 kHz adalah disebabkan resonans. Bolt M6 sepanjang 20 mm digunakan sebagai penyerap getaran dinamik dan dipasang pada permukaan motor untuk mengurangkan hingar pada 6 kHz. Penyerap getaran dinamik menyerap getaran sebanyak 20% hingga 86% pada permukaan motor dan pengurangan aras tekanan bunyi sebanyak 12 dB(A) dapat dicapai. Ia juga berkesan pada lokasi lain pada motor dan juga pada semua kelajuan operasi. Penyerap getaran dinamik telah terbukti untuk mengurangkan hingar elektromagnetik daripada motor induksi kelajuan boleh ubah.

**ATTENUATION OF ELECTROMAGNETIC ACOUSTIC NOISE
FROM A VARIABLE SPEED INDUCTION MOTOR
BY USING DYNAMIC VIBRATION ABSORBER**

ABSTRACT

Tonal electromagnetic acoustic noise radiated from variable speed induction motor can be annoying to human operator. Occurring at high frequency, it often occurs at multiples of the inverter switching frequency. Solutions for the noise attenuation have been generally by means of electromechanical design and pulse width modulation (PWM) strategy to remove harmonics leading to noise generation. Dynamic vibration absorber (DVA) as an alternative solution was implemented in this research. Spectral test revealed that the input electromagnetic excitation has direct influence on the radiated electromagnetic acoustic noise from the induction motor. The multiples of 3 kHz harmonics in PWM spectrum was also present in the surface vibration and sound pressure spectrum. From experimental modal analysis and spectral test, it was found that the 6 kHz acoustic noise was due to forced vibration for speed of 1250 rpm and below. While at above 1250 rpm, the 3 kHz noise was due to resonance. A 20mm M6 bolt was used as DVA and attached to a point on the motor housing for targeted noise attenuation at 6 kHz. The DVA was able to absorb the surface vibration in the range of 20 to 86% and maximum sound pressure level reduction of 12 dB (A) was achieved. It was also effective at other locations on motor as well as at different operating speed. The DVA was thus proven to be a feasible method for electromagnetic noise attenuation in induction motor.

CHAPTER 1

INTRODUCTION

1.1 Overview

Induction motor is the most widely used motor for industrial applications (Sahay and Pathak, 2006). It is generally used to drive pumps, compressors, conveyor belts and fans. Apart from being low cost, its popularity is also due to its ruggedness and excellent reliability in various operating conditions. Figure 1.1 shows the construction of an induction motor. The main components of the induction motor that are responsible for torque generation are the cage rotor and stator.

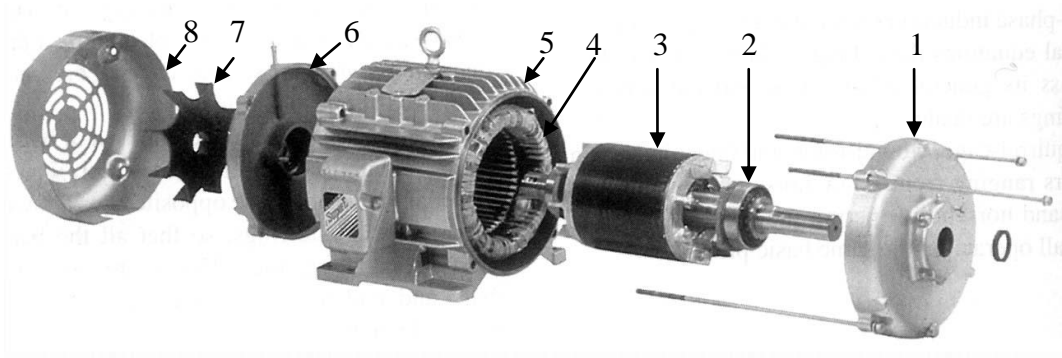


Figure 1.1 Exploded view of an induction motor. (1-Front end shield, 2 - Bearing, 3 – Cage rotor, 4 - Stator, 5 – Housing, 6 – Rear end shield 7- Cooling Fan, 8- Fan Cowl) (Wildi, 2002)

The induction motor produces its motion from the interaction of magnetic fields from both rotor and stator. Alternating current (AC) power supply to the stator coils produces rotating magnetic field around the stator. A second rotating magnetic field is then induced on the rotor bars of the squirrel cage. This two opposing magnetic field subsequently leads to the rotor's motion. Improving the advantage of the induction further for industrial use is the variable speed operation capability.

Using an inverter, the voltage and frequency of AC power supply can be controlled and thus a precise regulation of speed and torque is achieved.

While the induction motor is able to provide excellent motion drive, it has been known to produce acoustic noise which can be annoying to human exposure. The acoustic noise being emitted by an induction motor can be classified into three main categories: aerodynamic noise, mechanical noise and electromagnetic noise. Three different types of acoustic noise and its source are summarized in Table 1.1.

Table 1.1 Various types and source of acoustic noise from a variable speed induction motor (Gieras et al., 2005)

| Type | Source | Noise Characteristics |
|-----------------|---|------------------------------|
| Aerodynamic | Cooling fan airflow | Broadband |
| Mechanical | Ball bearing defects Bent shaft Rotor unbalance Shaft misalignment | Tonal |
| Electromagnetic | Electromagnetic force harmonics Phase unbalance Slotting effects Magnetic saturation Unbalanced magnetic pull | Tonal |

All these three different types of noise source combines to produce overall sound pressure level emitted by the motor. In aerodynamic noise, air turbulence induced by the cooling fan interacts with the motor housing to create flow induced noise. With increasing motor speed, the aerodynamic noise also increases. Mechanical noise occurs at discrete frequencies and depends on the motor speed as well. Unlike the aerodynamic and mechanical noise, there are many sources that lead to the electromagnetic noise. These different sources lead to numerous harmonics in the air gap flux density between rotor and stator. This in turn leads to periodic

fluctuations radial magnetic forces which deforms the stator. The radial deformation is what leads to the electromagnetic acoustic noise (Gieras et al., 2005).

The electromagnetic noise emanating from inverter driven induction motor is generally a high frequency acoustic noise. This unpleasant high frequency noise is narrow band or tonal in nature. Unlike the broadband noise in which the acoustic spectrum is spread over a range of frequency, the tonal noise generally occurs at discrete frequencies. Psychoacoustics research has indicated that tonal acoustic noise is subjectively more annoying than broadband noise (Kryter, 1968). Typical electromagnetic acoustic noise from a variable speed induction motor occurs at frequencies from 1000 Hz to 20,000 Hz. These frequencies are generally multiples or harmonics of various design parameters of the induction motor such as inverter switching frequency, number of stator and rotor slots and line frequency. Although human hearing ranges from 200 Hz to 20,000 Hz, human ears are more sensitive to the frequency range between 1000 Hz and 5000Hz (May, 2000). Realizing the sensitivity at this region, narrow frequency bands of electromagnetic noise within and nearby this frequency range is to be avoided. Generally, the aerodynamic and mechanical noise will mask the electromagnetic noise. However in certain cases, the electromagnetic acoustic noise can be the most dominant source of noise. For example, electromagnetic acoustic noise is more perceivable in light rail vehicle with traction motor (Le Besnerais et al., 2009a). Thus, the solution for electromagnetic acoustic noise is crucial.

The research and development in electric motor noise abatement was largely driven by strict industrial regulations throughout the world. Realizing that acoustic noise is one of the occupational health hazard, the motor noise limit is regulated by International Electrotechnical Commission (IEC). Figure 1.2 shows the standards for

maximum permissible sound power levels for a IEC squirrel cage induction motor.

The noise limit is based on the rated power output and number of poles.

| Rated speed n_N (rev/min) | $n_N \leq 960$ | | | $960 < n_N \leq 1320$ | | | $1320 < n_N \leq 1900$ | | | $1900 < n_N \leq 2360$ | | | $2360 < n_N \leq 3000$ | | |
|-----------------------------------|---|-------|-------|-----------------------|-------|-------|------------------------|-------|-------|------------------------|-------|-------|------------------------|-------|-------|
| Methods of cooling | IC01 | IC411 | IC31 | IC01 | IC411 | IC31 | IC01 | IC411 | IC31 | IC01 | IC411 | IC31 | IC01 | IC411 | IC31 |
| (simplified code) ^b | IC11 | IC511 | IC71W | IC11 | IC511 | IC71W | IC11 | IC511 | IC71W | IC11 | IC511 | IC71W | IC11 | IC511 | IC71W |
| | IC21 | IC811 | IC81W | IC21 | IC811 | IC81W | IC21 | IC811 | IC81W | IC21 | IC811 | IC81W | IC21 | IC811 | IC81W |
| | IC8A1W7 | | | IC8A1W7 | | | IC8A1W7 | | | IC8A1W7 | | | IC8A1W7 | | |
| | c | d | d | c | d | d | c | d | d | c | d | d | c | d | d |
| Rated output P_N (kW or kVA) | Maximum permissible sound power level L_{WA} (dB) | | | | | | | | | | | | | | |
| $1 \leq P_N \leq 1.1$ | 73 | 73 | | 76 | 76 | | 77 | 78 | | 79 | 81 | | 81 | 84 | |
| $1.1 < P_N \leq 2.2$ | 74 | 74 | | 78 | 78 | | 81 | 82 | | 83 | 85 | | 85 | 88 | |
| $2.2 < P_N \leq 5.5$ | 77 | 78 | | 81 | 82 | | 85 | 86 | | 86 | 90 | | 89 | 93 | |

Figure 1.2 Maximum permissible Sound Power Levels in Decibels for IEC Squirrel

Cage Induction motors (Toliyat and Kliman, 2004)

Solutions for electromagnetic noise mitigation for variable speed induction motor can be generally divided into two main methods: electromechanical design and pulse width modulation (PWM) strategy. The electromechanical design solution looks into the various geometrical design parameters of the induction motor. Examples include rotor-stator slot number combination (Kobayashi et al., 1997), stator slot opening width (Le Besnerais., 2009b) and rotor skew angle (Nau, 1997). This parameter has to be taken into account at the early stage of the design before manufacturing the motor. In PWM strategy, the PWM waveform from the inverter is optimized such that time harmonics of the magnetic flux density is minimized (Timar and Lai, 1994). Examples include ultrasonic switching (Gilliam et al., 1988), random PWM (Habetler and Divan, 1991) and pulse frequency modulation (PFM) (Ertan and Simsir, 2004).

Structural modification as a method to attenuate annoying acoustic noise has a potential to reduce the electromagnetic noise as well. In structural modifications, the vibration response of the structure can be altered by shifting the resonance or

changing the dynamic performance parameters. Various methods for structural modifications include mass modifications, selection of materials, stiffness alteration and vibration absorber addition (Kundra and Nakra, 1997). Structural modification as means to mitigate noise has been investigated for gearbox housing noise (Inoue et al., 2002) and drum brake squeal (Hamid et al., 2013).

In this research, the use of dynamic vibration absorber (DVA) to attenuate electromagnetic noise is investigated. DVA is a passive vibration control method whereby a secondary mass attached to a troublesome primary mass. The secondary mass natural frequency needs to be similar to the frequency of force excitation in order for primary mass vibration reduction (Mehta, 2012). The reduction should lead to reduction of the noise as well. DVA application has been popularly used for vibration control and the only reported use for acoustics control has been for aircraft cabin noise (von Flotow, 2000). It has not been reported to be used for noise control of electric motor and it is thus worth investigating on an induction motor in this research.

1.2 Problem Statement

Solutions for electromagnetic noise for induction motor have been largely focused on electromechanical design and PWM strategy. Various possibilities to optimize this two methods have reached its limit due to a range of tradeoffs such as sacrificing electrical efficiency and manufacturing costs. Moreover, there is a limit to the maximum noise level reduction achievable by each method. DVA as an alternative means to mitigate the electromagnetic acoustic noise is thus evaluated.

1.3 Motivation

Due to the electrical nature of the electromagnetic noise generation, the solution for electromagnetic noise has been tackled from electrical engineering point

of view. The current solutions available revolve around controlling the source of harmonics in the magnetic field between rotor and stator. From mechanical engineering standpoint, the electromagnetic noise problem can be solved by applying the solution at the receiver end by attaching a DVA on the motor to absorb and reduce the surface vibration that leads to acoustic noise. This research work is thus motivated by the need to solve the problem in an alternative way.

1.4 Objective

The main objective of this research is to evaluate the effectiveness of DVA to suppress tonal electromagnetic acoustic noise from variable speed induction motor

1.5 Contributions

The first contribution of this research is to investigate the correlation between the input electromagnetic excitation and the radiated electromagnetic acoustic noise. Though literature had mentioned that the frequency content of PWM has influence on the acoustic noise, but there is no available experimental data to show clearly the causal relationship. Through various noise and vibration characterization, this research thus shows the causal relationship between the input electromagnetic excitation and output electromagnetic acoustic noise.

The second and most important contribution is the investigation into the feasibility of DVA to suppress electromagnetic acoustic noise. The precedence of electromechanical design and PWM strategy has narrowed the scope for electromagnetic acoustic noise solution by various researchers. This research thus investigated an alternative solution.

1.6 Scope

The research is limited to experiments on motor noise and vibration characterization and DVA implementation. Basic noise and vibration characterization experiments such as spectral test, modal analysis and ODS was performed. PWM waveform tracing to determine the frequency content of electromagnetic excitation was conducted. Prior to DVA implementation, modal analysis on candidate DVA was carried out to obtain the suitable DVA. During implementation, effectiveness of DVA at various location, axis and speed was investigated.

1.7 Outline

This thesis is divided into five chapters which are introduction, literature review, methodology, results and discussions and conclusions. Chapter one presents basic idea of this research. A brief introduction to induction motor and electromagnetic noise is introduced. Problem statements, motivation, objectives, contributions, scope and outline are stated. Chapter two examines further into the literature on the electromagnetic noise generation mechanism and various solutions for noise suppression method. This chapter also presents the theory of DVA. Chapter three reports the methodology for various experiments for noise and vibration characterization and also implementation of DVA on the motor structure. In chapter four, results from the characterization and DVA implementation is presented. Finally, chapter five concludes all the findings from this research.